INTEGRATION OF OPTOELECTRONIC COMPONENTS WITH LTCC (LOW TEMPERATURE CO-FIRED CERAMIC) MICROFLUIDIC STRUCTURE

Karol Malecha

Wrocław University of Technology, Faculty of Microsystem Electronics and Photonics, Janiszewskiego 11/17, 50-372 Wrocław, Poland
(✉ karol.malecha@pwr.wroc.pl, +48 71 355 4822)

Abstract

Investigations on integration of optoelectronic components with LTCC (low temperature co-fired ceramics) microfluidic module are presented. Design, fabrication and characterization of the ceramic structure for optical absorbance is described as well. The geometry of the microfluidic channels has been designed according to results of the CFD (computational fluid dynamics) analysis. A fabricated LTCC-based microfluidic module consists of an U-shaped microchannel, two optical fibers and integrated light source (light emitting diode) and photodetector (light-to-voltage converter). Properties of the fabricated microfluidic system have been investigated experimentally. Several concentrations of potassium permanganate ($KMnO_4$) in water were used for absorbance/transmittance measurements. The test has shown a linear detection range for various concentrations of heavy metal ions in distilled water. The fabricated microfluidic structure is found to be a very useful system in chemical analysis.

Keywords: LTCC (low temperature co-fired ceramics), microfluidic, absorbance, CFD (computational fluid dynamics).

1. Introduction

The term 'microfluidic system' first appeared in the beginning of 1990 [1]. It is referring to a very small device which has characteristic dimensions in the range from tens of micrometers to single centimeters. Thanks to so small dimensions, the microfluidic system can handle a liquid or gas sample in the micro- or nanoliter volume range [2]. The main idea in microfluidics is very similar to that which is known from the computer industry. In 1971 thanks to the progress in semiconductor technology the big vacuum tube-based computing machines were replaced by very small transistor-based microprocessors. Generally the main idea in microfluidics is the same. It relies on replacing the big and complicated apparatus used in analytical chemistry with small microfluidic systems [3]. These systems are also called micro-total analysis systems (µTAS) or lab-on-chip (LOC) devices. In the beginning, the microfluidic systems were fabricated using silicon technology. However, due to high costs of the materials and technological equipment used for silicon micromachining, new materials and technologies suitable for microfluidics were sought. Nowadays polymer [4, 5], PCB (printed circuit board) [6, 7] and LTCC (low temperature co-fired ceramics) [8-10] technologies are used for fabrication of microfluidic structures.

The LTCC is a well known microelectronic technology. It has been developed in the 80s of the XXth century. Since then the LTCC technology has been used for fabrication of multilayer ceramic substrates. A typical LTCC structure is composed of several dielectric tapes covered by a network of conductive lines and thick-film passives. Conductive and passive layers are deposited on LTCC in a "green" (not fired) state using the standard screen-printing method. After screen-printing, ceramic tapes are stacked together in proper order and

---

are laminated. During the lamination process LTCC layers are pressed in an isostatic or uniaxial press with high pressure (up to 20 MPa) and at elevated temperature (up to 90°C). In the next step the laminated LTCC module is co-fired in a conveyor or box furnace according to a two-step thermal profile. During the co-firing process the flexible "green" LTCC tape is converted to rigid, solid dense material. In the first step of the thermal treatment (up to 500°C) solvents and organic binders are removed. In the second step temperature is increased to 850-900°C. During this step the LTCC laminate is densified. In the consequence of organics evaporation and densification the fired LTCC shrinks about 0.2-15% in the x- and y-direction and about 10-32% in the z-direction. Shrinkage values can vary for various LTCC green tape systems. After the co-firing process the active and passive electronic components can be placed on the top or bottom surface of the LTCC substrate using standard wire bonding, SMT (surface mounting technology) or flip-chip assembly.

The LTCC is a composite material. It consists of ceramics (45%), glass (40%) and an organic binder (15%). The organics binds and controls the viscosity of the LTCC material before the co-firing process. A glass frit binder reduces the processing temperature and makes LTCC compatible with thick-film technology. The LTCC material has a few interesting features which make this material almost ideal for fabrication of microfluidic structures. Green ceramic tape can be easily and precisely machined in order to fabricate channels, cavities, chambers or other microfluidic structures [11, 12]. Precise microfluidic, micromechanical and microelectronic structures with characteristic dimension in the range from 50 µm to single centimeters can be fabricated in green LTCC tape using hot embossing [13, 14], laser cutting [15-17], mechanical milling [8, 18] techniques. Moreover, a fired LTCC material is chemically resistant and chemically inactive [19, 20].

A LTCC microfluidic module with integrated optoelectronic components is presented in this paper. This module is built of an U-shaped microfluidic channel integrated with a light emitting diode (LED), photodetector and two optical fibers. The principle of operation of the LTCC microfluidic module is based on light absorption by a liquid sample. The green light from the LED is transmitted by optical fiber to the microfluidic channel. Light is partially absorbed by molecules of the flowing analyte. The non-absorbed light is transmitted through a second optical fiber to the photodetector. A photodetector converts the light signal into a voltage signal which is used for determination of the concentration of the analyte using Beer-Lambert's law:

$$A = -\log\left(\frac{I}{I_0}\right) = \varepsilon \cdot c \cdot l \qquad (1)$$

where: I_o and I are intensities of the light, c is the molar concentration (in M), ε is the molar absorptivity (in cm^{-1}M^{-1}) and l is the optical path length (in cm). It can be noticed that for the same conditions of measurement (same optical path length and molar absorptivity of the measured solution) absorbance is proportional to the concentration of the considered chemical in the particular solution. Similar microsystems made from silicon and glass [21], polymer [22] and LTCC [9] technology have been described recently. However, those microsystems were using external laboratory light sources and detection equipment which cannot be integrated with final structures. The main objective of the presented experiments was to investigate the possibility of integration of low-cost optoelectronic components with the LTCC microfluidic structure.

2. Numerical simulations

It is well known that geometry of the microfluidic structures has an effect on the functionality of the final device. In order to investigate the behavior of the fluid inside the

LTCC module, numerical simulations were made. A computational fluid dynamics (CFD) analysis was performed for a two-dimensional, steady state, incompressible, laminar flow. A model fluid with properties similar to water was chosen (density $\rho = 10^3$ kg/m^3; dynamic viscosity $\mu = 10^{-3}$ Pa·s). The U-shaped microfluidic structure was built of three components: the inlet channel, outlet channel and an absorption cell. All components were 420 µm high, 500 µm wide and 1 cm long. The fluid flow equations (Navier-Stokes) were solved using a commercial ANSYS® software package.

For all investigated cases, a uniform flow rate was applied at the inlet. A zero velocity condition at the inlet in the direction normal to the inlet flow was applied as well. Zero velocities in the x and y directions were applied along the microfluidic structure walls. Zero relative pressure was applied at the outlet. Two cases were taken into account: first, when the axial misalignment of the fiber end face to fluidic channel was equal to 150 µm (Fig. 1) and second, when the optical fiber was located inside the microchannel to a length of 150µm (Fig. 2). In the first case, local disturbances (recirculation areas) of fluid flow near the optical fiber were noticed. This phenomenon was proportional to the magnitude of misalignment. In the second case, the presence of the optical fiber inside the absorption cell did not have an effect on fluid flow conditions. The CFD simulations show that on the one hand the misalignment between the optical fiber and fluidic channel can create fluid recirculation or zero-flow regions. The fluid recirculation region precludes effective pumping out of the analyte from the absorption cell. Moreover, the recirculation regions have a tendency to accumulate impurities and air bubbles which can have an effect on proper function of the final device. On the other hand if an optical fiber is located inside a very narrow fluidic channel (~150 µm), it can block the fluidic channel. The results of the CFD computations for an ideal case are presented in Fig. 3. However, in spite of a perfect match between the optical fiber and fluidic channel, the calculated fluid distribution showed two small fluid recirculation regions. The recirculation regions were formed in the corners of the microfluidic structure. In order to eliminate this phenomenon, a new geometry of the microfluidic was proposed. The absorption cell of the new microfluidic structure was two times wider and truncated at an angle of 45°. Results of the CFD computations for the microfluidic structure with new geometry are presented in Fig. 4. The new geometry avoided fluid recirculation formation within the absorption cell space.
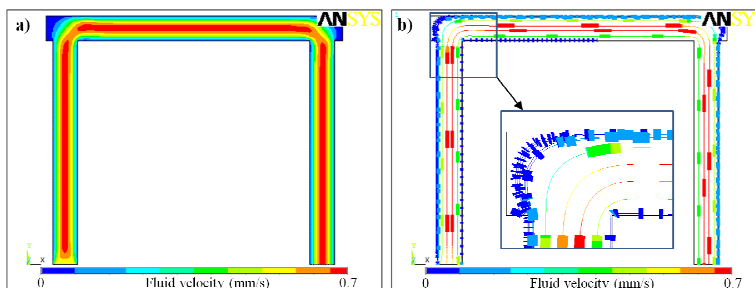

Fig. 1. Results of CFD simulations for a microfluidic structure with misaligned optical fibre to fluidic channel by 150 µm: (a) velocity field and (b) fluid trajectories.
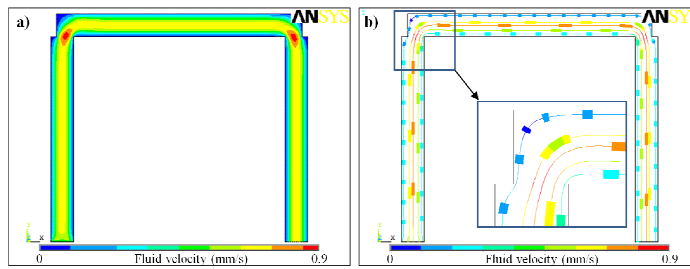
Fig. 2. Results of CFD simulations for a microfluidic structure with an optical fibre placed inside the fluidic channel to a length of 150 µm: (a) velocity field and (b) fluid trajectories.
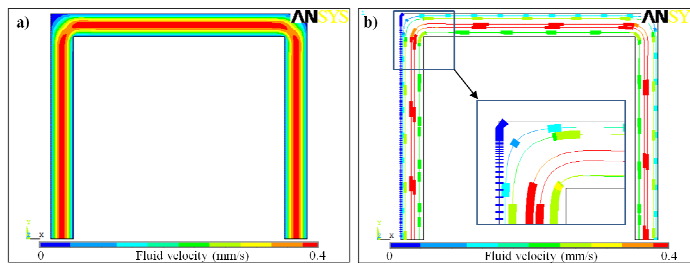

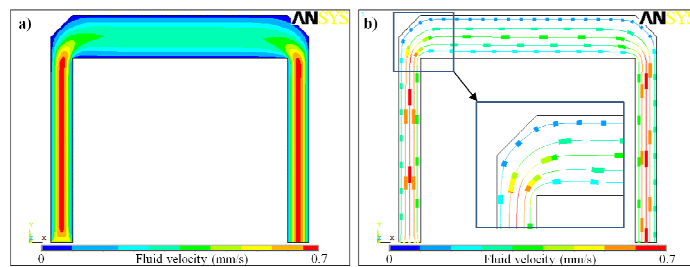Fig. 3. Results of CFD simulations for an ideal case: (a) velocity field and (b) fluid trajectories.

Fig. 4. Results of CFD simulations for a microfluidic structure with new geometry of the absorption cell: (a) velocity field and (b) fluid trajectories.

3. Technology

The LTCC microfluidic structure was designed on the grounds of the performed CFD analysis. A schematic view of the device is presented in Fig. 5. It consists of an inlet and outlet channel, an absorption cell, two channels for optical fibers and two cavities for the light source and a light detector. In order to ensure a 1 cm distance between optical fibers, a special construction of the LTCC microfluidic structure was proposed. The channels for optical fibers were about two LTCC tapes higher than the absorption cell. The created threshold allows to precisely position the optical fibers. The construction of the threshold for optical fiber positioning is presented in Fig. 6. The real model of the LTCC microfluidic structure was made of fourteen DP951 P2 LTCC tapes (DuPont, UK). The thickness of each LTCC tape was equal to 140 µm after firing. All LTCC layers used for construction of the microfluidic structure are presented in Fig. 7. Layer (a) consists of cuts for the photodetector and holes for electrical interconnections. Layer (b) defines cavities for the LED and photodetector. Channels for optical fibers are made in layer (c) and (e). Microfluidic channels are cut in layer

(d). Channels, cavities and alignment holes were cut in green LTCC tapes using a Nd-YAG laser (Aurel NAVS 30). Conductive lines made of PdAg (DP 6146) were deposited through a 325 mesh steel screen using a standard screen-printing method. After laser cutting and screen printing, all LTCC tapes were stacked together and laminated in an isostatic press. The lamination process was performed at a pressure of 10 MPa, temperature of 70°C for 10 minutes. In the next step, the LTCC laminate was co-fired in a programmable chamber furnace (Nabertherm L3/S) according to the standard two-step profile with a peak temperature at 880°C.
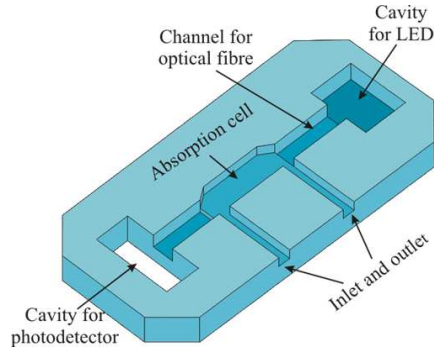

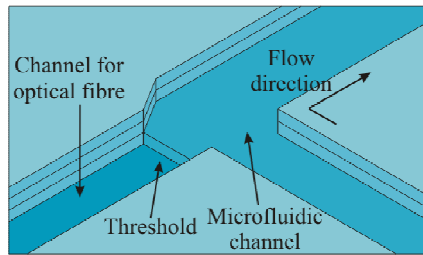Fig. 5. Schematic view of the LTCC microfluidic structure (without cover).

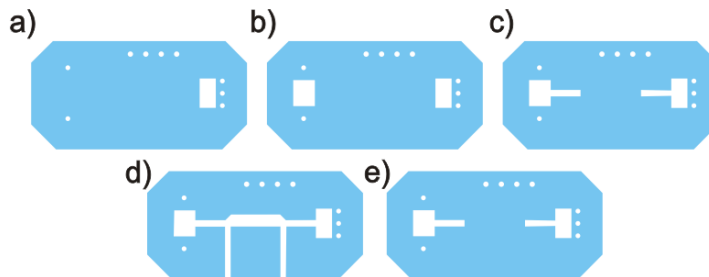Fig. 6. Construction of the threshold for optical fiber alignment.

Fig. 7. Design of the layers to construct the LTCC microfluidic structure: a) orifices for photodetector and electrical interconnections, b) orifices for LED, photodetector and electrical interconnections, c), e) openings for LED, photodetector, electrical interconnections and channels for optical fibers, d) openings for LED, photodetector, electrical interconnections, microfluidic channels and channels for optical fibers.

After the co-firing process two PMMA optical fibers were glued to the LTCC microfluidic structure. The LED (KA-4040SGC, Kingbright), photodetector (TSLG 257, TAOS) and passives were mounted on the surface of the LTCC module using a standard soldering

technique. Finally, the fluidic inlet and outlet made of steel pipes were glued using epoxy resin. The final LTCC microfluidic structure is presented in Fig. 8.
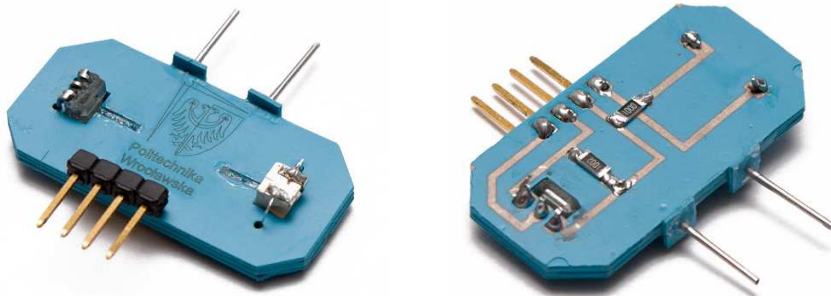

Fig. 8. LTCC microfluidic structure with integrated optoelectronic components.

Proper alignment of the microfluidic channels, cavities for optoelectronic components and other spatial structures inside the LTCC module after isostatic lamination and co-firing processes was examined using non-destructive X-ray microscopy. Fig. 9 depicts X-ray images of the fired LTCC-based microfluidic system. As can be seen in Fig. 9, microfluidic structures and optoelectronic components are alignment properly. Moreover, there is no deformation or delamination of the microfluidic structures.

4. Results and discussion

Properties of the fabricated LTCC microfluidic structure were examined experimentally. It is well known that the LED luminance can change with temperature. In order to determine the variation of the LED temperature during its operation, thermographic measurements were done. Temperature changes were measured by an infrared (IR) thermo-scanner. Results of the thermographic measurements are presented in Fig. 10.
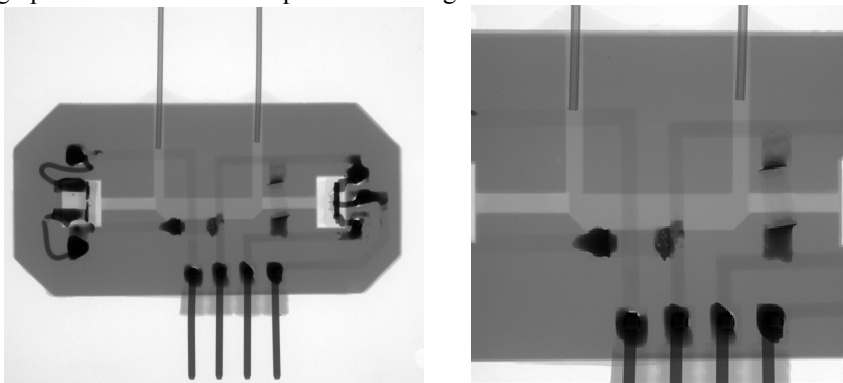

Fig. 9. X-ray images of the LTCC microfluidic structure.

According to the transient measurements, the time necessary to reach a stable temperature of 30°C was equal to about 10 minutes. After 10 minutes the temperature of the LED remained more or less the same.
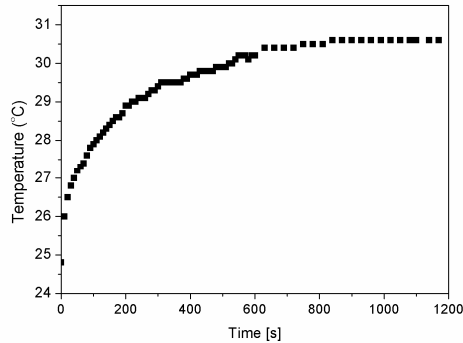
Fig. 10. Temperature changes of the LED as a function of time measured by the thermographic system
(LED current equal to 20 mA).

Several concentrations of potassium permanganate ($KMnO_4$) in the range from 6 to 38 µM were prepared. Potassium permanganate after dissolving in distilled water gave a purple solution which absorbed light at a wavelength $\lambda_{max} = 535$ nm. Concentrations of the test solution were pumped to the LTCC microfluidic structure by a syringe pump (Perfursor® Space, Braun). Measurements for each concentration were made in 5-minute intervals. The electroluminescent diode was supplied by a square-shaped signal (max. current equal to 20 mA) in order to eliminate the influence of external light source constant radiation. Green light from the LED ($\lambda_{max} = 565$ nm, $\Delta\lambda_{1/2} = 30$ nm) was transmitted via an input optical fiber to the absorption cell. The light passing through the test solution was partially absorbed. The magnitude of the absorbed light was proportional to the concentration of the examined test solution according to Beer'a-Lambert law. The non-absorbed light was transmitted to the photodetector. The applied photodetector (TSLG 257) has maximum spectral responsivity at a wavelength of 524 nm with the halfwidth equal to 47 nm. It converts the light intensity to the output voltage signal. Therefore, it was possible to measure the concentration of $KMnO_4$ utilizing the following formula:

$$A = \log\left(\frac{I_0}{I}\right) = \log\left(\frac{U_0}{U(c)}\right) \tag{2}$$

where U_o is the output voltage for distilled water (in V) and $U(c)$ is the output voltage measured for test solution (in V) with concentration c (in M). Measurement of the output voltage level was performed using a lock-in amplifier. Measured time responses and the calibration curve of the LTCC microfluidic structure are presented in Fig. 11a and 11b, respectively. The absorbance measurements performed in the LTCC microfluidic structure have shown that it was possible to observe changes of the output signal. The signal-to-noise ratio was quite high, the output signal has good repeatability without drift in time. The linear detection range of the LTCC microfluidic structure for concentrations of the $KMnO_4$ was ranging from 6.3 to 32 µM. The slope of the calibration curve was equal to 0.08. For concentrations above 32 µM of the $KMnO_4$ the output signal approached saturation and did not fit to a linear curve. Beer-Lambert's law relies on the assumption that every particle in the solution absorbs light independently and is not affected by other particles. However, this assumption is not fulfilled in a highly concentrated solution. In such solution the absorbing particles can be placed along the same optical path, therefore, some particles can be in the shadow of other particles.

Performed measurements of the LTCC microfluidic structure with integrated opto-electronic components have shown that the used light source introduced enough light into the

optical fiber and into the absorption cell. The high numerical aperture (NA = 0.5) and core diameter of the used polymeric optical fibers enable to achieve a good light-coupling coefficient from the LED into the optical fiber and from the optical fiber to the absorption cell and photodetector.
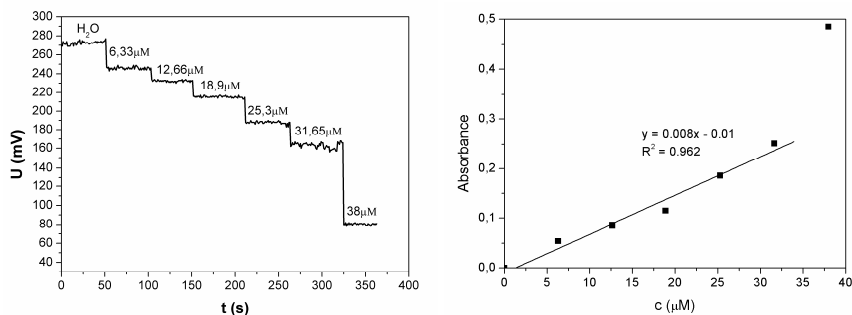

Fig. 11. Dynamic response and calculated calibration curve of the fabricated LTCC-based microfluidic structure.

5. Conclusions

A LTCC microfluidic structure with integrated optoelectronic components was designed, fabricated and positively tested. The geometry of the fluidic structures was designed according to results of numerical computations. The performed CFD analysis of fluid flow avoided formation of fluid recirculation in the area of the absorption cell. On the basis of CFD results a real microfluidic structure was fabricated. The LTCC microfluidic structure with integrated optoelectronic components allowed to perform measurements of absorbance. The test solution of $KMnO_4$ in distilled water was used in order to measure the absorbance. The absorbance measurements shown that the light source used introduced sufficient light into the optical fiber and the absorption cell. Therefore, it was possible to measure changes of the output signal for various concentrations of the test solution. The results of light absorbance measurements indicate a quite linear dependence of the test solution concentration in the range from 6 to 32 µM, thus the designed microfluidic structure can be applied as concentration sensors after some calibration effort.

The possibility of integration of fluidic structures and optoelectronic components has shown that LTCC technology can be a very promising alternative for fabrication of microfluidic structures.

Acknowledgment

References

[1]   Gravesen, P., Branebjerg, J., Søndergård Jensen, O. (1993). Microfluidic – a review. *J. Micromech. Microeng.*, (3), 168-182.

[2] Wautelet, M. (2001). Scaling laws in the macro-, micro- and nanoworlds. *European Journal of Physics*, (22), 601-611.

[3] Manz, A., Graber, N., Widmem, H.M. (1990). Miniaturized total chemical analysis system: a novel concept for chemical sensing. *Sens. Actuators B*, (1), 244-248.

[4] Duffy, D.C., Cooper McDonald, J., Schueller, O.J.A., Whitesides, G.M. (1998). Rapid prototyping of microfluidic systems in poly(dimethylsiloxane). *Anal. Chem.*, (70), 4974-4984.

[5] Fujii, T. (2002). PDMS-based microfluidic devices for biomedical applications. *Microelectronic Engineering*, (61-62), 907-914.

[6] Merkel, T., Graeber, M., Pagel, L. (1999). A new technology for fluidic Microsystems based on PCB technology. *Sens. Actuators A*, (77), 98-105.

[7] Läritz, Ch., Pagel, L. (2000). A microfluidic pH-regulation system based on printed circuit board technology. *Sens. Actuators A*, (84), 230-235.

[8] Gongora-Rubio, M.R., Espinoza-Vallejos, P., Sola-Laguna, L., Santiago-Avilés, J.J. (2001). Overview of low temperature co-fired ceramics tape technology for meso-system technology (MsST). *Sens. Actuators A,* (89), 222-241.

[9] Golonka, L.J., Roguszczak, H., Zawada, T., Radojewski, J., Grabowska, I., Chudy, M., Dybko, A., Brzózka, Z., Stadnik, D. (2005). LTCC based microfluidic system with optical detection. *Sens. Actuators B*, (111-112), 396-402.

[10] Ibáñez-Garcia, N., Martinez-Cisneros, S., Valdés, F., Alonso, J. (2008). Green-tape ceramics. New technological approach for integrating electronics and fluidics in microsystems. *Trends in Analytical Chemistry*, (27), 24-33.

[11] Malecha, K., Golonka, L.J. (2008). Microchannel fabrication process in LTCC ceramics. *Microelectronics Reliability*, (48), 866-871.

[12] Malecha, K., Golonka, L.J. (2009). Three-dimensional structuration of zero-shrinkage LTCC ceramics for microfluidic applications. *Microelectronics Reliability*, (49), 585-591.

[13] Andrijasevic, D., Smetana, W., Zehetner, J., Zoppel, S., Brenner, W. (2007). Aspects of micro structuring low temperature co-fired ceramic (LTCC) for realization complex 3D objects by embossing. *Microelectronic Engineering*, (84), 1198-1201.

[14] Rabe, T., Kuchenecker, P., Schulz, B. (2007). Hot embossing: an alternative method to produce cavities in ceramic multilayer. *Int. J. App. Ceram. Technol.*, (4), 38-46.

[15] Kita, J., Dziedzic, A., Golonka, L.J., Zawada, T. (2002). Laser treatment of LTCC for 3D structures and elements fabrication. *Microelectronics International*, (19), 14-18.

[16] Nowak, D., Miś, E., Dziedzic, A., Kita, J. (2009). Fabrication and electrical properties of laser-shaped thick-film and LTCC microresistors. *Microelectronics Reliability*, (49), 600-606.

[17] Markowski, P. (2011). Thick-film photoimageable and laser-shaped arms for thermoelectric microgenerators. *Microelectronics International*, (28), 43-50.

[18] Barlow, F., Wood, J., Elshabini A., Stephens, E.F., Feeler, R., Kemner, G., Junghansm J. (2009). Fabrication of precise fluidic structures in LTCC. *Int. J. App. Ceram. Technol.*, (6), 18-23.

[19] Bembnowicz, P., Małodobra, M., Kubicki, W., Szczepańska, P., Górecka-Drzazga, A., Dziuban, J., Jonkisz, A., Karpiewska, A., Dobosz, T., Golonka, L.J. (2010). Preliminary studies on LTCC based PCR microreactor. *Sens. Actuators B*, (150), 715-721.

[20] Thelemann, T., Fisher, M., Groß, A., Müller, J. (2007). LTCC-based fluidic components for chemical applications. *Journal of Microelectronics and Electronic Packaging*, (4), 167-172.

[21] Bargiel, S., Górecka-Drzazga, A., Dziuban, J., Prokaryn, P., Chudy, M., Dybko, A., Brzózka, Z. (2004). Nanoliter detectors for flow systems. *Sens. Actuators A*, (115), 245-251.

[22] Grabowska, I., Sajnoga, M., Juchniewicz, M., Chudy, M., Dybko, A., Brzózka, Z. (2007). Microfluidic system with electrochemical and optical detection. *Microelectronic Engineering*, (84), 1741-1743.